End-to-end Cardiac Ultrasound Simulation for a Better Understanding of Image Quality

Alexandre Legay, Thomas Tiennot, Jean-François Gelly, Maxime Sermesant, Jean Bulté

End-to-end Cardiac Ultrasound Simulation for a Better Understanding of Image Quality

Authors' own version : The final authenticated version is available online at https://doi.org/10.1007/978-3-030-39074-7_18.

Alexandre Legay[1], Thomas Tiennot[2⋆], Jean-François Gelly[1], Maxime Sermesant[2], and Jean Bulté[1]

[1] GE Parallel Design SAS, Sophia-Antipolis, France jean.bulte@ge.com
[2] Inria, Université Côte d'Azur, Sophia-Antipolis, France
maxime.sermesant@inria.fr

Abstract. Ultrasound imaging is a very versatile and fast medical imaging modality, however it can suffer from serious image quality degradation. The origin of such loss of image quality is often difficult to identify in detail, therefore it makes it difficult to design probes and tools that are less impacted. The objective of this manuscript is to present an end-to-end simulation pipeline that makes it possible to generate synthetic ultrasound images while controlling every step of the pipeline, from the simulated cardiac function, to the torso anatomy, probe parameters, and reconstruction process. Such a pipeline enables to vary every parameter in order to quantitatively evaluate its impact on the final image quality. We present here first results on classical ultrasound phantoms and a digital heart. The utility of this pipeline is exemplified with the impact of ribs on the resulting cardiac ultrasound image.

Keywords: Ultrasound, Cardiac Modelling, Probe Design, Image Quality.

1 Introduction

Simulation of medical images has been an active research area for several years. Synthetic images are often associated with ground-truth information on the underlying anatomy and function used to generate the images [2].

Therefore, it enables to evaluate image processing algorithms [4] as well as generating data for machine learning. Approaches vary from simulating the whole physics of medical image acquisition to warping an existing image, including all the intermediate combinations.

⋆ Alexandre Legay and Thomas Tiennot are co-first authors, they contributed equally to this work.

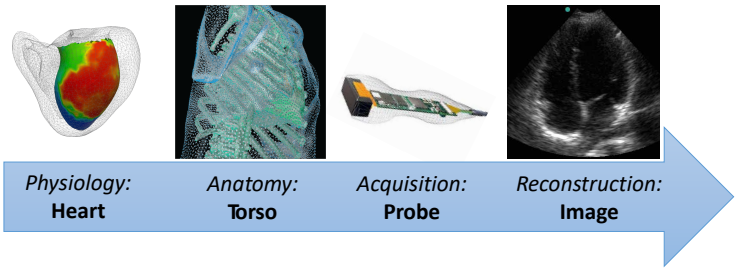

Fig. 1. End-to-end modelling pipeline for echocardiography simulation.

In this work, we developed an original approach integrating a full simulation pipeline in order to leverage image simulation for image quality understanding (see Fig. 1). It includes detailed modelling of both human anatomy and ultrasound probe. This is the first time that such simulations are directly linked to probe parameters in order to understand better the relationship between these parameters and image quality. Moreover, some modifications of our anatomy numerical model such as addition, removal and resizing of organs, tissues and bones can be easily done and their impacts studied.

2 Cardiac Model

Modelling cardiac electromechanical activity has been an active research area for the last decades, as can be seen in references from recent reviews like [3]. Simulating 3D cardiac function enables to completely control the multi-physics phenomena including electrophysiology, biomechanics and blood flows. In the context of simulating ultrasound images, cardiac modelling enables to generate ground-truth data on position, motion, strain, velocities, etc. for the subsequently generated images.

In this work, we used a detailed segmentation of the heart available from the Visible Human Project [1]. We only simulated a static ultrasound image as a proof-of-concept of the whole pipeline. See Fig. 2 for the anatomy of the heart and the imaging slice used in this manuscript.

3 Torso Model

Once cardiac activity has been simulated, it is necessary to include it within a digital representation of the human torso, as the heterogeneities within the thorax are responsible for an important part of artifacts and echogenicity problems. We used a detailed segmentation of the human torso from the Visible Human project. It enables to introduce various structures of the human body and to see their influence on the simulated images.

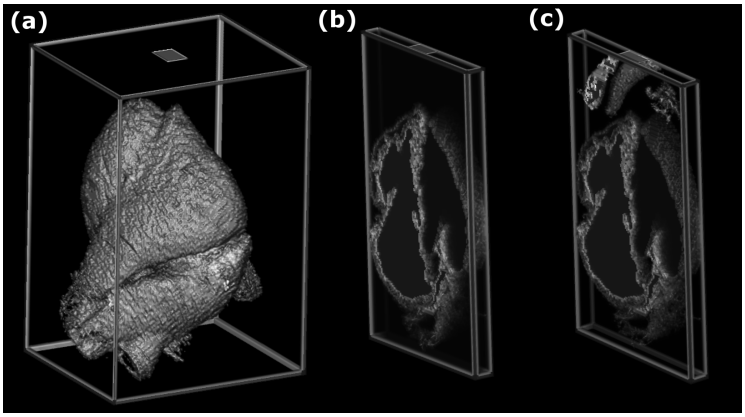

Fig. 2. (a) 3D cardiac model and probe location. Corresponding 2D imaging slice without (b) and with the rib cage (c).

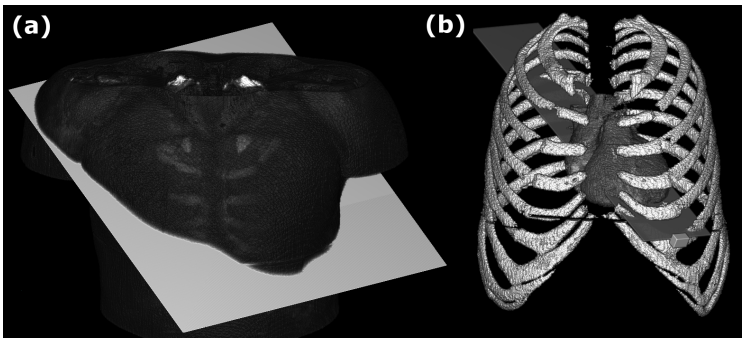

Fig. 3. 3D torso model (a) and imaging plan (b).

4 Probe Model

Numerical simulations were performed using k-Wave, a k-space pseudospectral method-based solver [8]. The k-Wave toolbox solves coupled first-order acoustic equations. An ultrasonic source, a medium (heterogeneous or not) and a sensor should be defined within these equations. In our case, the ultrasonic source and the sensor are modeled by the 3Sc-RS sector probe designed for cardiac applications (General Electric Healthcare, Illinois, USA.) The k-Wave solution enables the definition of every physical property of the probe: the number of piezoelectric elements and their width, height and spatial positioning. It also allows the complete tuning of the emission and reception beam-forming with the definition of the focal distance in azimuth, the focal distance in elevation as well as transmitted and received apodizations.

We could have chosen Field II [5] [6] but k-Wave was selected for two main reasons. Firstly, it defines the medium of propagation as a grid where the physical

parameters influencing the propagation of the ultrasonic wave (speed of sound, density, absorption, acoustic non-linearity parameter B/A) can be defined inhomogeneously. In contrast, Field II defines it as a collection of scatterers defined by their positions and amplitudes. The final objective of this project was to study the anatomical causes of the image degradation so we decided to keep a simulation tool that allowed us to model these physical parameters precisely. Secondly, k-Wave offers a free parallel version on GPU whereas the parallel version of Field II is not open-source. Considering that we can use a GPU cluster for the project, k-Wave was chosen.

The input signal used to drive the piezoelectric elements was made of n sinusoidal periods ($0.5 < n < 3$) at a central frequency $f_0 = 1.7$ MHz. Results are presented with harmonic imaging (reception at $2f_0 = 3.4$ MHz).

5 Reconstruction

B-mode imaging consists in a gray-scaled representation of the echogenicity of the tissue. A mechanical wave is sent in the body and is back-scattered because of the speed of sound and density heterogeneities. k-Wave models the medium of propagation as a speed of sound and a density distribution mapped on a Cartesian grid. Other parameters like absorption or the non-linearity coefficient B/A can also be defined on this grid. This medium of propagation can be defined in 2D or 3D. The choice made should be studied case by case.

To do 2D modeling is equivalent to ignore the influence of the planes parallel to the imaging plane. Clearly, this hypothesis is directly satisfied if the medium of propagation is invariant along the elevation direction of the probe. The 3D case can be considered to verify this hypothesis or in all other situations where the parallel planes are important. 3D simulations can be made using an optimized version of k-Wave running on Graphics Processing Unit (GPU) which drastically reduces the computation time (up to 10 times faster than the original code on Matlab). This version is currently unavailable in 2D and 2D simulations can only be run in Matlab (The MathWorks Inc., Massachusetts, USA.) Nonetheless, the memory available on current GPU limits the size of the Cartesian grid that has to be modeled. This essential drawback will be discussed in Section 7.

6 Results

6.1 Theoretical validation of the Point Spread Function (PSF)

The Point Spread Function (PSF) of any imaging system is its response to a point source. For B-mode imaging, such a source consists in an infinitesimally small region where the speed of sound and the density distributions slightly differ from the rest of the medium. Recovering the physical PSF of the 3Sc sector probe within our pipeline is a key step towards its validation.

We here present this validation for the 2D case (see the Discussion section for its extension in 3D). Nonetheless, the spatial steps and the number of points

used for the simulation grid have a direct impact on the quality of the PSF recovering. In fact, the maximum frequency that can propagate and be solved in the numerical simulations is inversely proportional to the smallest spatial step used. Here we chose a 2008 x 2008 2D grid with respectively 90 μm and 75 μm spatial steps. The corresponding dimensions of the modeled medium are 180 mm (depth) and 150 mm (width). Thus the maximum frequency respecting the Nyquist theorem of two points-per-wavelength is $f_{max} = 8.6$ MHz.

The emitted signal is made of 2.56 sinusoidal cycles at $f_0 = 1.7$ MHz. No apodization or filtering is applied to this signal. The imaging sequence is composed of 120 angles between $-30°$ and $30°$. The modeled medium consists in an homogeneous speed of sound of $c_0 = 1540$ m.s^{-1} and an homogeneous density of $d_0 = 1035$ kg.m^{-3}, apart from the point source where $c_1 = 1600$ m.s^{-1} and $d_1 = 1040$ kg.m^{-3}. This point source is made of one single point of the simulation grid aligned with the middle of the simulated probe and placed at 100 mm.

An intensity profile is extracted from the 100 mm-radius circle centered in the middle of the 1D-transducer. A log compression is applied and relative intensities are displayed with respect to the orientation of the point with the probe (Fig. 4). Both profiles are normalized to the maximum intensity obtained in the simulation. The simulated profile is in excellent agreement with the theoretical expectation. The agreement (in particular for the five main lobes) is nonetheless sufficient to validate the PSF recovery within our simulations. This result also confirms the relevance of the spatial steps chosen in our study.

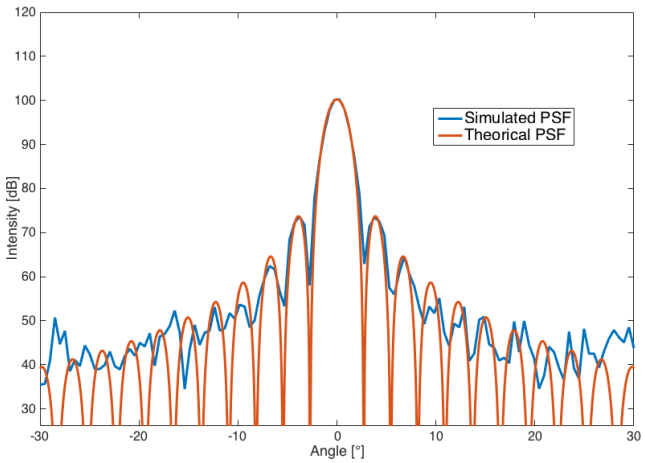

Fig. 4. Simulated (blue line) and theoretical (red line) PSF.

6.2 Experimental validation on an acoustic phantom

The theoretical validation of the PSF has been completed by an experimental validation of the simulations. B-mode images of an acoustic phantom 403GS LE (Gammex Inc., Middleton, Wisconsin, USA.) have been acquired with the 3Sc probe connected to a commercial console Vivid S70 (General Electric Healthcare, Illinois, USA.) Contrary to more complex modeling (like in Section 6.3), simulating the phantom in 2D is still relevant since it is invariant in one direction (height direction). Elevation imaging plane is thus not impacted by structural heterogeneities. The grid parameters used for the theoretical validation are conserved (90 μm and 75 μm spatial steps, 2008 x 2008 points, 180 x 150 mm dimensions). Here we chose to use an emission frequency at 2.3 MHz and to focus on harmonic imaging (reception at 4.6 MHz). The spatial steps upper defined guarantee 3 points-per-wavelength at 4.6 MHz.

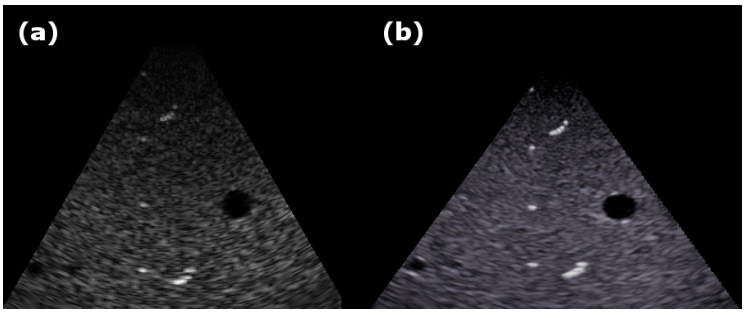

Fig. 5. (a) Simulated B-mode image of the Gammex phantom. (b) Corresponding Experimental B-mode image of the Gammex phantom acquired with the 3Sc probe on the Vivid S70 console.

Figure 5 provides both the experimental and simulated B-mode images. The agreement between the two images is fairly good. Both pin targets and anechoic cysts' acoustic behaviours are caught up within our simulation (respectively higher and lower reflection than the background). Speckle pattern of the phantom background is also well recovered.

6.3 Numerical simulation of a cardiac image in apical view

An echographic image of the numeric heart phantom described in Section 2 has been simulated. In that case, the elevation dimension has to be modeled leading to the realization of simulations in 3D. The imaging slice used here is shown in Fig. 2(b). The grid dimensions are 1024 x 512 x 64 (depth x width x heigth) with respectively 189 μm, 219 μm and 200 μm spatial steps. These grid dimensions correspond to the largest grid that can fit the memory of GPU currently available and used in this study. The corresponding dimensions of the modeled medium

are 193 mm (depth), 112 mm (width) and 15 mm (height). Thus, the maximum frequency respecting the Nyquist theorem of two points-per-wavelength is $f_{max} = 4.1$ MHz in depth, $f_{max} = 3.4$ MHz in width and $f_{max} = 2.3$ MHz in height. In that case we study fundamental imaging at $f_0 = 2.8$ MHz. The simulated image is provided in Fig.6 (a). Myocardium as well as both ventricles and atria are well recovered. Speckle pattern is coherent near the probe but spatial resolution is slightly too high further away from it (see Discussion). Such an image can be obtained in about 30 minutes.

Finally we provide preliminary results showing how our pipeline can be used to study the impact of anatomical structures on image quality. We have added a modelling of the rib cage on our previous imaging slice (see Fig. 2(c)). The corresponding simulated image is provided in Fig. 6(b). One can see that the rib cage causes a shadowing of the right ventricle that makes disappear its walls. Ribs also cause a blurring of left atrium and left ventricle. This leads to an apparent thickening of the mitral valve as well as a distortion of the atria's shape. These results are coherent with physicians experience during clinical exams.

Nonetheless both images of Fig. 6 display a numerical artefact because of the limited number of points along the height direction. As mentioned above the maximum frequency that satisfies the Nyquist theorem in that direction is $f_{max} = 2.3$ MHz which is lower than our fundamental frequency at emission ($f_0 = 2.8$ MHz). Thus a bright point can be seen around the coordinate (100,60) on both images. This is due to aliasing and the non-propagation of frequencies above $f_{max} = 2.3$ MHz.

7 Discussion

The accuracy of our simulations has been demonstrated both theoretically and experimentally in the 2D case where smaller spatial steps can be used with reasonable computational costs. The extension to 3D simulations is still limited by the memory size currently available on GPU. Video cards used in this study (GeForce GTX 1080 Ti, NVIDIA Corporation, California, USA) have a memory of 11 GB which can contain a grid made of 2^{25} points. Cardiac simulations presented in this study are designed to meet the best trade-off between this memory constraint, the spatial steps needed to propagate relevant frequencies and the actual size of the medium to simulate. To do so, we had to increase the step size in the height direction leading to aliasing and poor spatial resolution far from the probe.

Nonetheless we believe these limitations will soon disappear. First, the memory available on GPU is rapidly increasing. Second, a discussion with the creators of k-Wave lets us think that a new version of the optimized code, distributed over several GPUs, will soon be available. This will lead to smaller computation times and will also allow running simulations on a far larger grid than today, therefore improving precision and complexity.

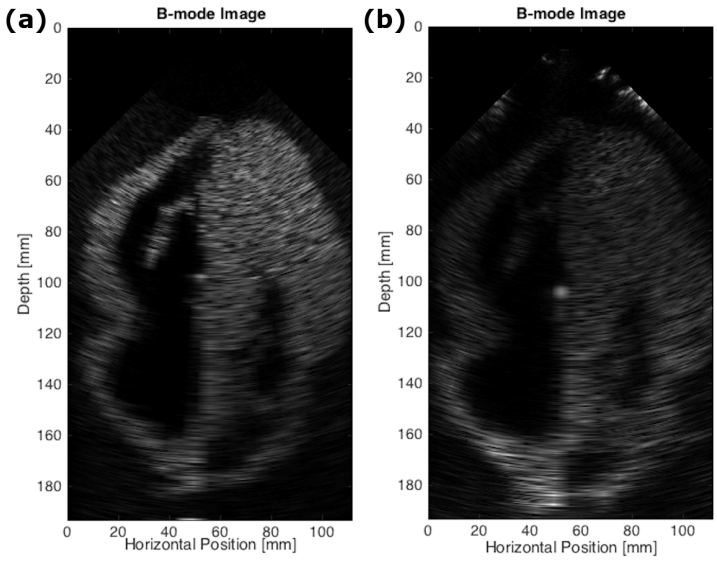

Fig. 6. Simulated B-mode image of the heart model without (a) and with (b) ribs within the imaging field.

For now, absorption and non-linearities are not taken into account. These two features can directly be set in k-Wave when defining the medium of propagation. Their addition will increase the accuracy of our pipeline.

Moreover, the propagation of shear-waves in bony structures like ribs would also have to be studied. The k-Wave toolbox provides a wave-equation solver based on a visco-elastic definition of the medium of propagation [7]. This solver has not been used in this study but its implementation should be straightforward.

Finally, the cardiac modeling could benefit from many add-ons related to many anatomic or functional diseases that have to be studied. Important computational improvements can even lead to a 4D (3 spatial dimensions and time) modeling of the heart. In such a case, complex dysfunctions like arrhythmia and their translation into an echographic image could be developed.

8 Conclusion

An end-to-end simulation pipeline including realistic cardiac, torso and ultrasonic probe modelling has been presented. The control over every simulation steps offers a great freedom for investigating the echographic image quality. The simulations' accuracy has been confirmed by recovering a theoretical PSF and the comparison of 2D simulations with experimental B-mode images of an acoustic phantom. Finally, simulated B-mode images of the heart model with and without the rib cage have been created to investigate its impact on the image quality. The inclusion of more advanced anatomical and physiological features together with

current computational improvements, making this simulation pipeline a useful tool to investigate the key aspects of image quality.

References

1. Ackerman, M.J.: The visible human project. In: 1998 IEEE International Ultrasonics Symposium. vol. 86, pp. 504–511 (1998)
2. Alessandrini, M., et al.: A Pipeline for the Generation of Realistic 3D Synthetic Echocardiographic Sequences: Methodology and Open-access Database. IEEE Transactions on Medical Imaging **34**(7) (2015)
3. Chabiniok, R., et al.: Multiphysics and multiscale modelling, data-model fusion and integration of organ physiology in the clinic: ventricular cardiac mechanics. Interface Focus **6**(2) (2016)
4. De Craene, M., et al.: 3D strain assessment in ultrasound (straus): A synthetic comparison of five tracking methodologies. IEEE Transactions on Medical Imaging **32**(9) (2013)
5. Jensen, J.: Field: A program for simulating ultrasound systems. Medical & Biological Engineering & Computing **34** (1996)
6. Jensen, J., Svendsen, N.B.: Calculation of pressure fields from arbitrarily shaped, apodized, and excited ultrasound transducers. IEEE Transactions on Ultrasonics, Ferroelectrics and Frequency Control **39** (1992)
7. Treeby, B.E., Jaros, J., Rohrbach, D., Cox, B.T.: Modelling elastic wave propagation using the k-wave matlab toolbox. In: 2014 IEEE International Ultrasonics Symposium. pp. 146–149 (2014)
8. Treeby, B.E., Jaros, J., Rendell, A.P., Cox, B.T.: Modeling nonlinear ultrasound propagation in heterogeneous media with power law absorption using a k-space pseudospectral method. Journal of the Acoustical Society of America **131**(6) (2012)